LUND UNIVERSITY

Understanding the Chemistry of Lead at a Molecular Level: The Pb(II) 6s6p Lone Pair Can Be Bisdirected in Proteins

Van Severen, Marie-Celine; Ryde, Ulf; Parisel, Olivier; Piquernal, Jean-Philip

Link to publication

Understanding the toxicology of lead at a molecular level: Pb(II) 6s lone pair can be bisdirected in proteins.

Marie-Céline Van Severen**, Ulf Ryde**, Olivier Parisel*, Jean-Philip Piquemal*

*Laboratoire de Chimie Théorique, UPMC, CC 137, 4 place Jussieu, 75252 Paris, Cedex 05, France and CNRS, UMR 7616, CC 137, 4 place Jussieu, 75252, Paris Cedex 05, France.

**Theoretical chemistry, Lund University, P.O. Box 124, 22100 Lund, Sweden.

Contact author: mc.vanseveren@gmail.com

ABSTRACT

Pb^{2+} complexes can attain several different topologies, depending of the shape of the Pb $6s6p$ lone pair. In this paper, we study structures with a bisdirected Pb lone pair with quantum mechanics (DFT) and QM/MM calculations. We study small symmetric Pb^{2+} models to see what factors are needed to get a bisdirected lone pair. Two important mechanisms have been found: First, the repulsion of the lone pair of Pb^{2+} with other lone pairs in the equatorial plan leads to a bisdirected structure. Second, a bisdirected lone pair can also arise thanks to interactions with double bonds, lone pairs, or hydrogen atoms (resembling hydrogen bond). Moreover, we have analysed Pb^{2+} sites in proteins and RNA (both for frozen and relaxed structure, and with sites saturated with water molecules) to see if a bisdirected lone pair can exist in an asymmetrical environment. Bisdirected lone pairs were encountered in several of them.

KEYWORDS
Bisdirected, RNA, QM/MM, ELF, Lead

The toxicity of lead is known since the antiquity and for mammals its ingestion results in the well-known disease saturnism. Experiments indicate that two types Pb^{2+} complexes exist: holodirected and hemidirected organizations (Figure 1)[1]. This structural difference is caused by the peculiar capably of the Pb *6s 6p* lone pair to adapt to the presence of ligands. Hemidirected complexes arise when Pb^{2+} spreads the ligands in one hemisphere, letting the lone pair to expand in the opposite direction. This extension of the lone pair can cause structural variations in the protein chelation site and perturbs its native structure, leading to possible loss of activity. When this is not possible, due to strong steric and electrostatic interactions between the ligands, holodirectional complexes are recovered and the lone pair looses its stereochemical activity.
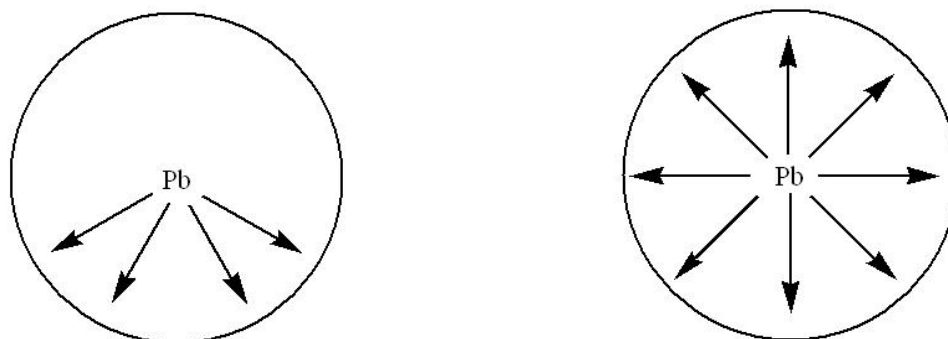
Hemidirected Structure

Figure 1: Schematic representation of hemi- and holodirected structures, where the arrows indicate location of ligands.

In a recent paper, we showed that the lone-pair organization can be even more complex: We observed a third possible organization of the *6s* lone pair, called bisdirected[2] (see Figure 2c). In this case, the lone pair is split in two hemispheres. Such topological structure was obtained when Pb was bound to a plane and symmetric molecule. We showed that the topological analysis with the electron localization function (ELF) is a powerful tool to localize and visualize the domain corresponding to the valence lone pair of Pb (V(Pb)). In this study, we address answer to several questions: When will the lone pair of Pb^{2+} be bisdirected? What factors favour this structure? Could such a topological structure exist within proteins where the symmetry and flatness are absent? To address such issues, we analyse Pb^{2+}-containing protein structures that are available in the protein data bank (PDB) using the ELF analysis coupled with DFT and combined quantum mechanical and molecular mechanical QM/MM calculations.
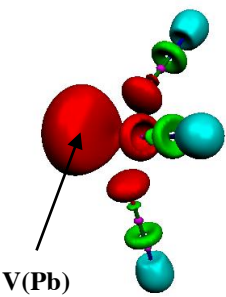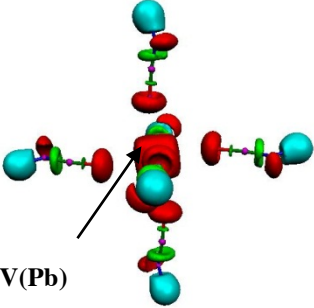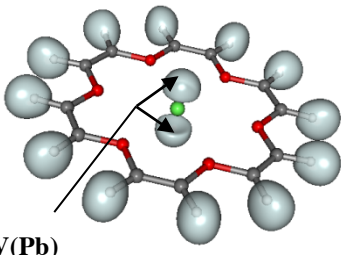
a) [Pb(HNC_O_)_3]^{2+}	b) [Pb(HNC_O_)_6]^{2+}	c) HCOH
Hemidirected structure	Holodirected structure	Bisdirected structure

Figure 2: Three different topological structures of the lone pair of Pb²⁺. (The red colour is used for a basin that belongs to only one atom, the green colour is used for basin shared by two atoms and the blue colour is for the hydrogen + the covalent bond H-X with X=any atoms. On the right the basin of Pb²⁺ and the basin of H are not coloured)

Results

In this article, we will study bisdirected Pb²⁺ *6s6p* lone pairs in various structures with the aim to understand where and why this topology arises. We will first study a series of model complexes to understand when bisdirected lone pairs arise. Then, we will study Pb²⁺ in protein structures to see if bisdirected structures are encountered in biological systems.

Bisdirected lone pairs in model complexes

Figure 2c shows a bisdirected lone pair in the complex of Pb²⁺ with the chelating ligand 1,4,7,10,13,16-hexaoxa-cyclooctadeca-2,5,8,11,14,17 hexaene (HCOH), which consists of six oxygen atoms alternating with six C=C double bonds. One can ask whether it is the oxygen atoms or the double bond that give rise to this bisdirected lone pair. To answer this question, we deleted the double bonds of HCOH replaced and the carbon atoms by hydrogen atoms (

a) H of H₂O are in the plane of the molecule	b) H of H₂O are out of the plane of the molecule

Figure 3). Thus, the complex is now formed by six water molecules with the oxygen atoms located in the same place as the oxygen atoms in HCOH in Figure 2c.
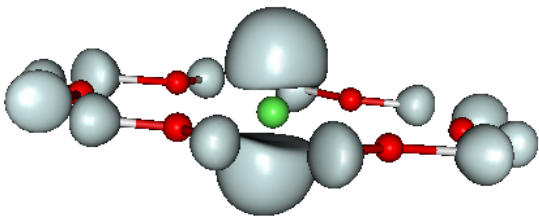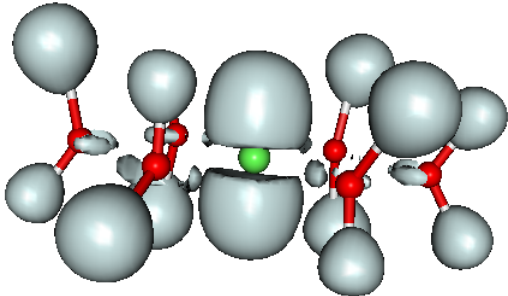

a) H of H₂O are in the plane of the molecule	b) H of H₂O are out of the plane of the molecule

Figure 3: ELF representation of HCOH replaced by six water molecules.

3

From the ELF analysis in Figure 3a, it is obvious that the lone pair of Pb^{2+} is still bisdirected. It seems that this structure is caused by the repulsion of the lone pairs of oxygen atoms creating a hole in the lone pair of Pb^{2+}. To exclude the possibility that the bisdirected structure is linked to the direction of the lone pairs of the oxygen atoms, another calculation was carried out with the hydrogen atoms directed vertically to plane with the Pb and O atoms (Figure 3b). However, the ELF analysis shows that the lone pair of Pb^{2+} is still bisdirected. This indicates that the Pb lone pair will be bisdirected in structures where some atoms induce repulsion in a plane.

Ligand	Pb(p)	O(p)	H(s)
HCOH	0.50	4.96	0.73
$(H_2O)_6$ planar	0.19	5.27	0.45
$(H_2O)_6$ perpendicular H	0.22	5.32	0.40

Table 1: NBO analysis of the bisdirected structures in Figures 2 and 3 for only one O and one H in the different system.

Table 1 shows electronic populations of the donor orbitals: $2p$ of O and $1s$ of H and the acceptor $6p$ orbitals of Pb^{2+}. As the 6s of Pb^{2+} is already full the occupation of 6p orbitals are important because they will receive the electron for the environment. It can be seen that the lone pair of Pb^{2+} in the HCOH complex has a higher population than in the complexes with water molecules. The oxygen orbitals of this complex have lower populations than the water complexes because of the more polar bonds in the water molecules. Consequently, the populations on the hydrogen atoms are higher in the HCOH complex than in the two water complexes. This is comprehensible, considering that in the HCOH ring there are more electrons available, thanks to double bonds, so the oxygen atoms take electrons form the hydrogen atoms in one case and from the C=C double bonds in the other case.

This example is not enough to settle why the bisdirected structure is observed. Further evidence can be obtained by using a molecule that does not cut the lone pair of Pb^{2+} in its middle. Therefore, we studied the $Pb(C_{16}H_{16}O_{16})^{2+}$ complex (complex A) in

a) Ball and stick representation	b) Side view	c) Top view

Figure 4.

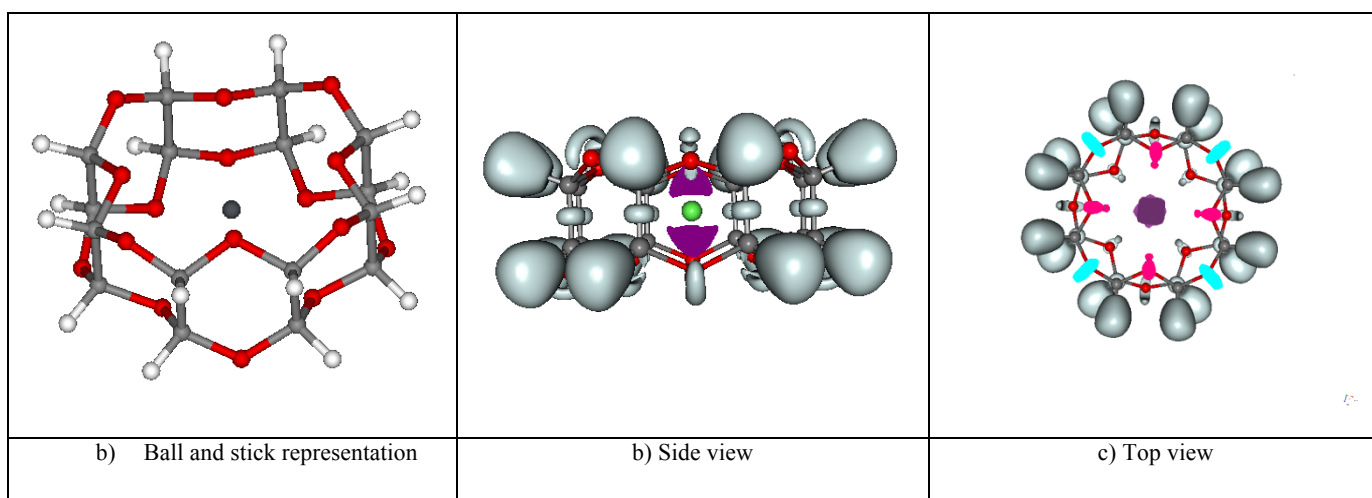| b) Ball and stick representation	b) Side view	c) Top view

Figure 4: Schematic and ELF representations of complex A. (Violet colour is for the basin of Pb^{2+}, the pink colour for the basin of the oxygens that point inside the cycle and the blue colour for the basin of oxygens that point outside the cycle.)

As can be seen from the ELF analysis, again the lone pair of Pb^{2+} is bisdirected. From Figure 4b, it can be seen that the ELFs form three plans, two formed by alternation of the oxygen and carbon atoms on the top and bottom of the ligand and a third one, in the middle of the ligand, formed by the C–C σ bonds. The bisdirected lone pair can be caused by two effects, viz. either the alignment of the lone pair of Pb^{2+} with the lone pairs of the oxygen atoms or the repulsion from the σ bonds. In Figure 4c, we have colour-coded the oxygen lone pairs depending on whether they point towards the Pb ion (pink) or out of the molecule (blue). This shows that the blue oxygen lone pairs do not interact with the lone pair of Pb^{2+}, because they point to the outside the molecule, whereas the pink oxygen lone pairs interact with the bisdirected lone pair on Pb.

To further understand this phenomenon, the ligand was cut in a similar manner as for the HCOH complex above, keeping only the eight pink oxygen atoms. An ELF analysis of the remaining $Pb(H_2O)_8$ complex was performed without any optimisation of the structure. The results in Figure 5 shows that a bisdirected lone pair was still found, indicating that the electronic structure is caused by the oxygen atoms, not by the σ liaisons.
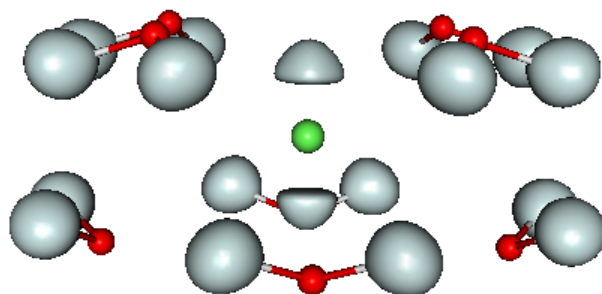
Figure 5: Complex A replaced by eight water molecules.

However, in our previous study, we found that a fully optimised $[Pb(H_2O)_8]^{2+}$ complex gave rise to a holodirected structure[3] (Figure 6). Comparing Figure 5 and Figure 6, it can be noted that the positions of the hydrogen atoms are different. Therefore, another ELF analysis was carried out after moving the hydrogen atoms in the same way as in Figure 5, keeping the oxygen atoms at their optimised positions. However, the results in Figure 7 show that the lone pair of Pb^{2+} is still holodirected.

Figure 6: ELF representation of [Pb(H₂O)₈]²⁺.	**Figure 7: ELF representation of [Pb(H₂O)₈]²⁺ with the H atoms oriented in the same way as in the complex in Figure 5.**
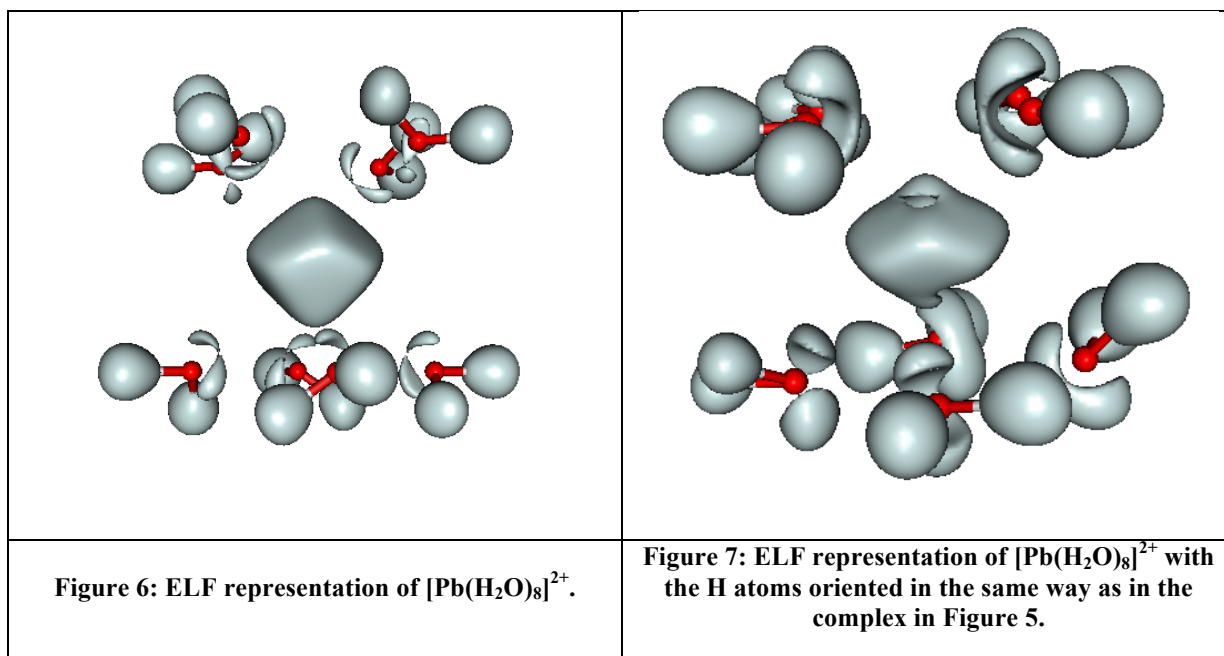
In fact, there is still another difference between Figure 5 and Figure 6, viz., the O1–Pb–O2 angle, where O1 = oxygen of the top plane and O2 = oxygen of the bottom plane. In the structure in Figure 5, this angle is 70°, whereas it is 92° for the structure in Figure 6. Therefore, we keep the structure of Figure 5 and increase the angle, still without any optimisation. From the ELF analysis in Figure 8, it can be seen that at 72°, the structure is still bisdirected. However, at 78°, the Pb lone pair starts to become a torus, in addition of being bisdirected. At 81°, we have clearly a torus and still a bisdirected structure. Finally at 89°, only a torus is observed. Thus, it seems that increasing the angle between the two plans induces a change in the interaction between oxygen and Pb lone pairs. This change induces a change in the shape of the Pb lone pair from bisdirected to a torus. Consequently, the formation of the bisdirected structure seems to be linked to the orientation of the oxygen lone pairs around the Pb²⁺ ion.
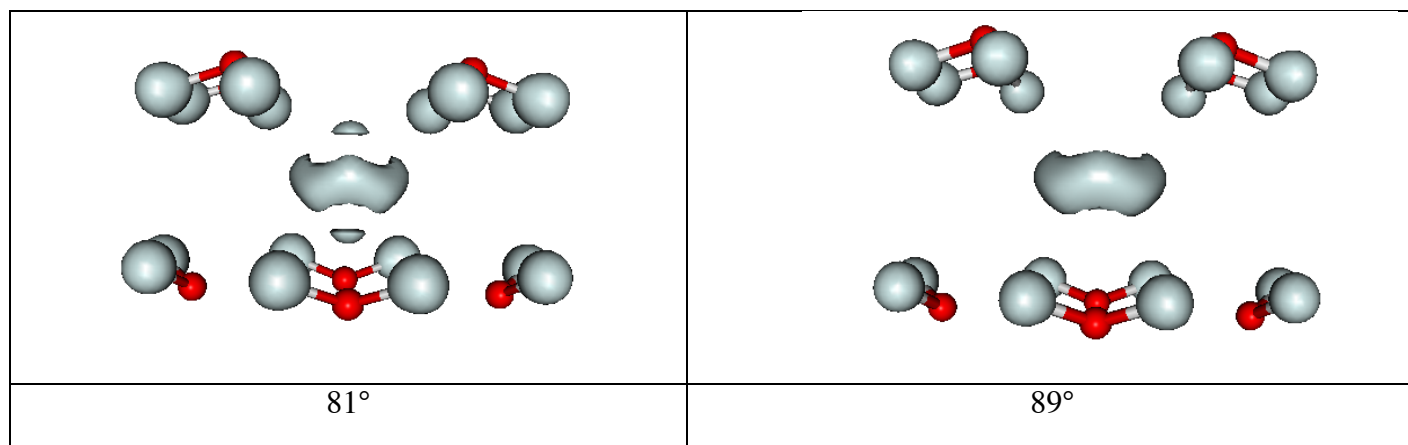

72°	78°

| 81° | 89° |
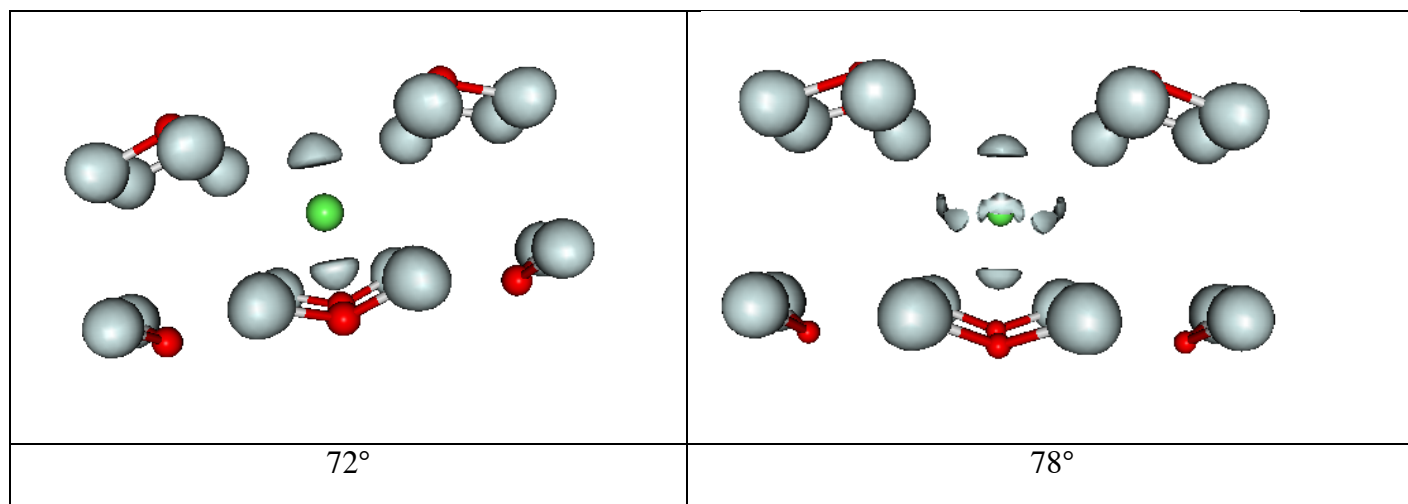
Figure 8: ELF analysis of complexes with different values of the O1-Pb-O2 angle. Note that the isosurface value is higher than the one used in Figures 5–7.

O1–Pb–O2 angle	Pb $6p^-$	Energy
69°	0.36	28
72°	0.38	16
78°	0.4	1
81°	0.43	0
89°	0.44	10

Table 2: NBO analysis and relative energies (kcal/mol) of complex A replaced by eight water molecules, increasing the O1-Pb-O2 angle.

The NBO analysis of these complexes in Table 2 shows that the Pb lone pair becomes more and more populated when the O1–Pb–O2 angle increases. Likewise, the energies decrease with this angle, except for 89°, because the complexes are not optimised. For the optimised $[Pb(H_2O)_8]^{2+}$ complex, the angle is 92° and the energy 94 kcal/mol lower than for the most stable complex in Table 2. Thus, the interactions between lead and ligands become more and more important while the angle increases.

Next, we studied the effect of the π bonds. First, we tested the $Pb(C_{18}H_{24})^{2+}$ complex (complex B) in Figure 9, which has three double bonds at the top and three double bonds at the bottom of the ligand. After optimisation, Pb^{2+} is at the centre of the chelate. An ELF analysis reveals that the structure is bisdirected (Figure 10). In this figure, we have colour-coded the π bonds in green and the lone pair of Pb^{2+} in red. This time, the carbon and Pb lone pairs are aligned, but the σ bonds of the C–C bonds are aligned with the hole of the lone pair of Pb^{2+}.
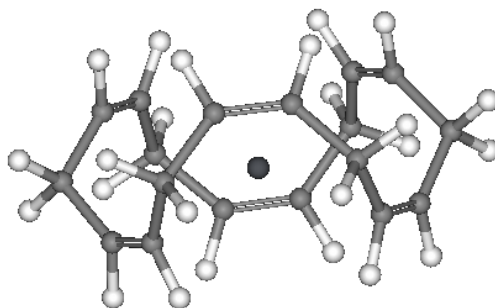

Figure 9: Pb^{2+} coordinated to the complex B.

| Top view of complex B | Bottom view of complex B |
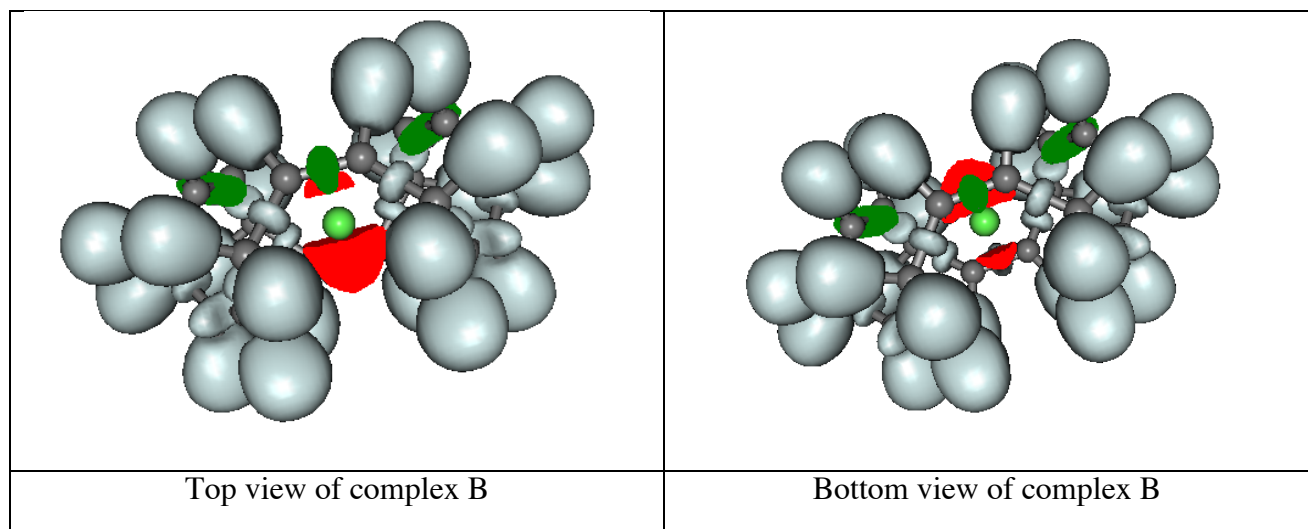
Figure 10: ELF representation of complex B. (The basin of Pb^{2+} is in red and the basin of oxygens in green)

To know which of those phenomena is responsible for the bisdirected shape, additional calculations were run. First, we removed the σ bonds, without any optimisation. The ELF analysis in Figure 11 shows that the π bonds are enough to give a bisdirected structure.

Figure 11: ELF representation of Pb^{2+} surrounding by six ethylene molecules.

Second, we removed the lower part of the ligand and keep only upper part of it, i.e. Pb and three ethylene molecules. The ELF analysis in Figure 12 shows that hemidirected structure is obtained, which illustrates that ligands on both sides of the Pb ion are needed to give a bisdirected structure.
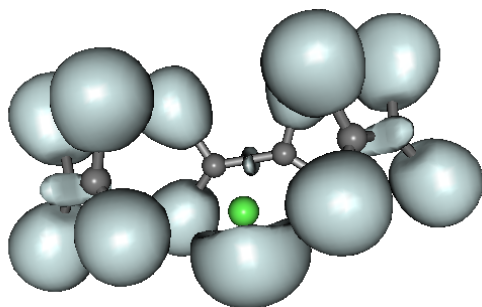
Figure 12: ELF representation of Pb^{2+} surrounding by three ethylene molecules.

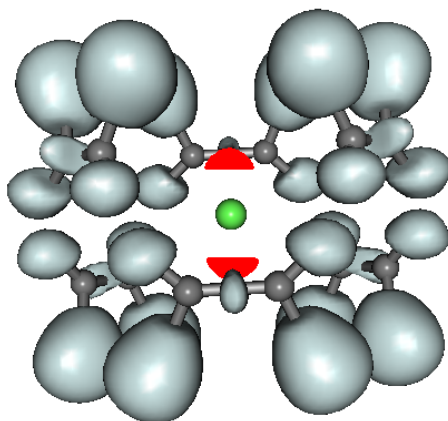Next, we tested a series of cyclic ligands constructed from merged benzene rings. The aim was to see what happens when the symmetry is broken by removing some of the carbon atoms. The whole system is optimized. The left part of Figure 13 shows Pb^{2+} surrounded by eight merged benzene rings. The ELF analysis reveals that the lone pair of Pb^{2+} is split in three: two bisdirected lobes and a torus-shape central lobe. One can see a clear alignment between the lone pair of Pb^{2+} and the π bonds of benzene.

| Pb(C$_{32}$H$_{16}$)$^{2+}$ | Pb(C$_{32}$H$_{18}$)$^{2+}$ |
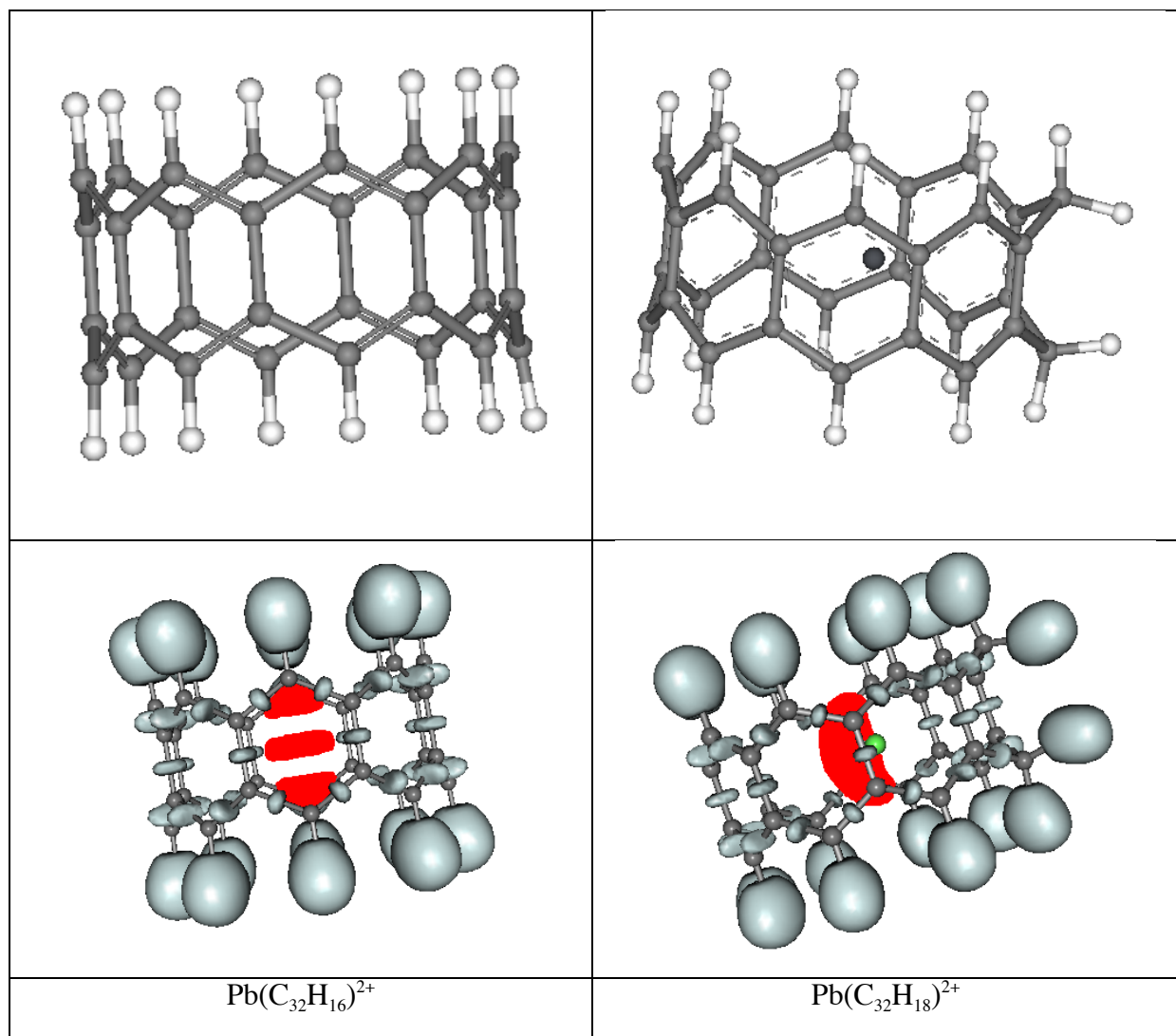
Figure 13: Schematic and ELF representations of the complex B and its corresponded hydrogenated.

However, if a pair of carbon atoms are saturated in one of the benzene molecules (Figure 13b), the Pb lone pair becomes hemidirected and the distance between Pb^{2+} and the two saturated carbons becomes shorter than the distances to the other carbon atoms.

Next, three benzenes have been removed leaving only five benzene rings (Figure 14a). In Figure 14b, the two first carbons on each side of the molecule have been removed and in Figure 14c the two next carbons on each side have been deleted. These systems are now opened and no optimization has been done: the aim is just to see how the lone pair reacts in different environment. This was followed by an ELF analysis. The results in Figure 14 show that the lone pair of Pb^{2+} is mainly vertically bisdirected and that the lone pair of Pb^{2+} is again aligned with the π bonds of C–C.

a) First cut, giving five benzene rings, $Pb(C_{22}H_{14})^{2+}$

b) Second cut, giving $Pb(C_{18}H_{14})^{2+}$ with three intact benzene rings

10

c) Third cut, giving Pb$(C_{14}H_{10})^{2+}$ also with three benzene rings
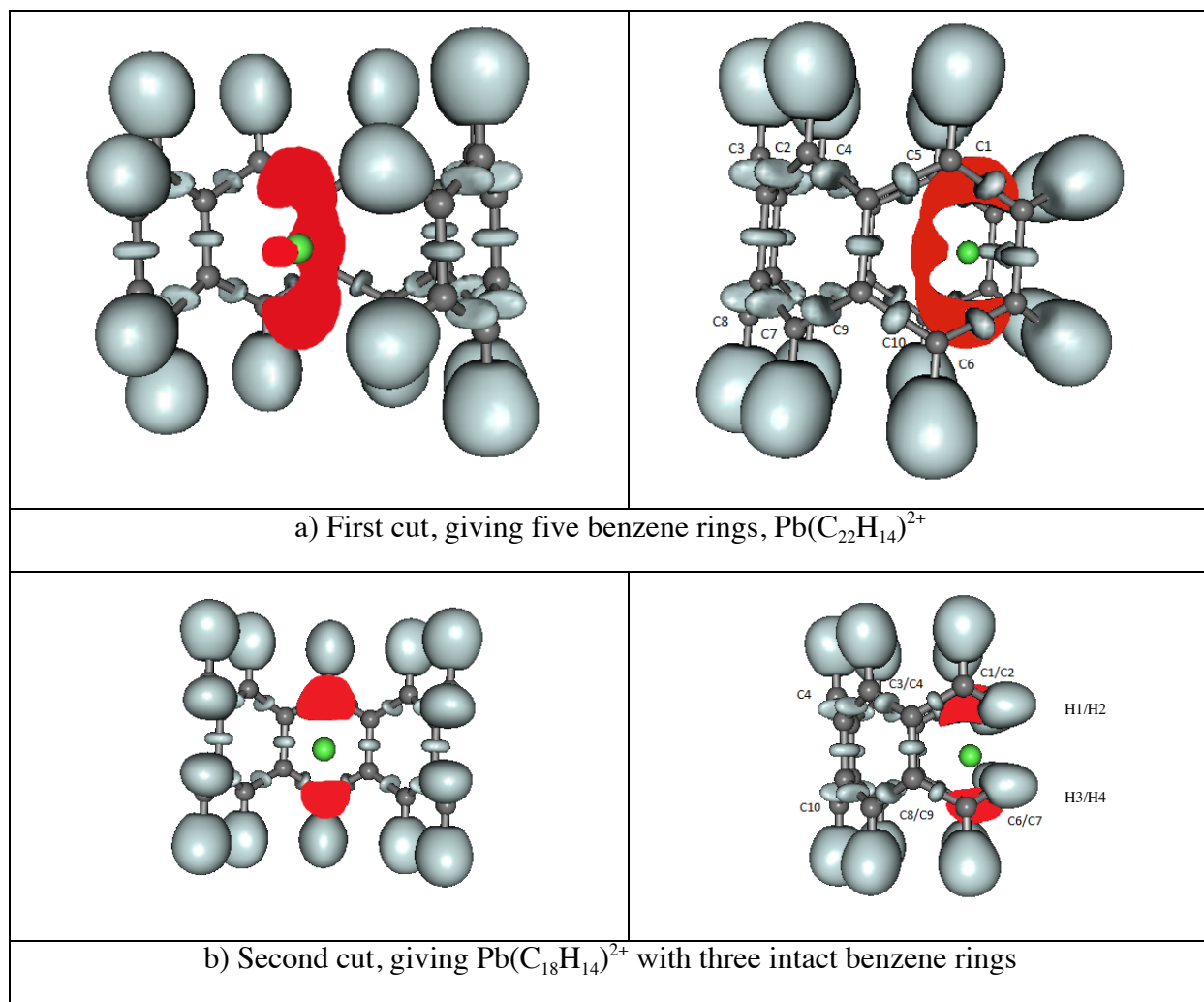
Figure 14: The complexes with cut merged benzene rings.

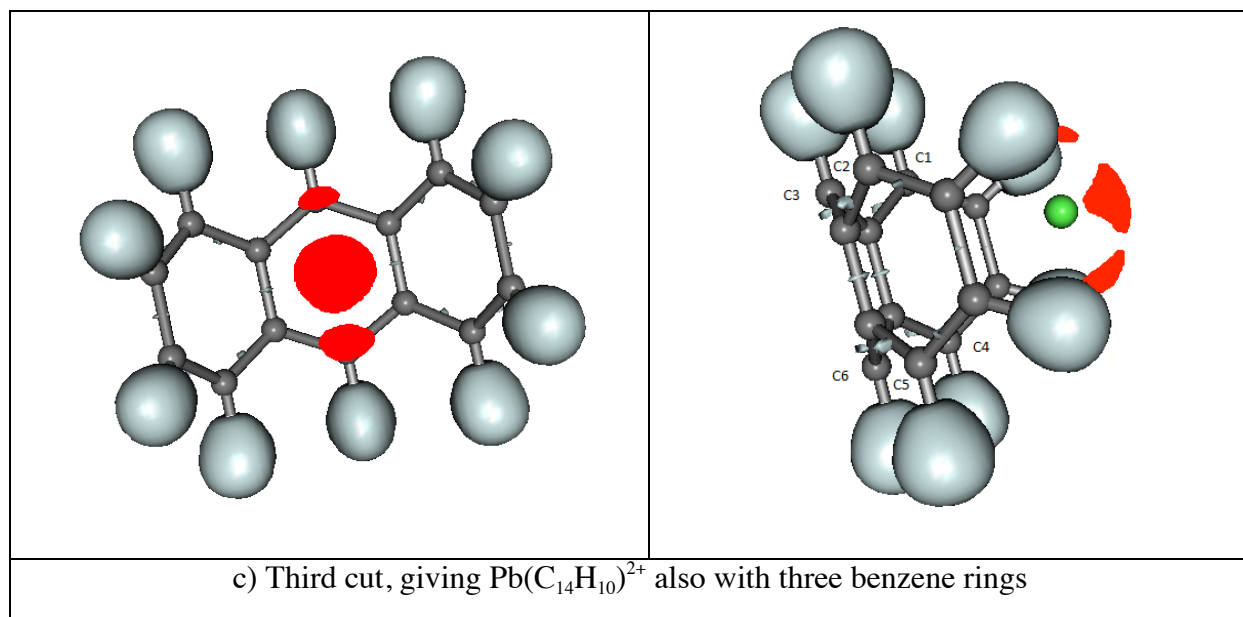Then, we removed two C atoms at each end of the ligand, giving three merged benzene rings with two CH$_2$ groups at each end. As can be seen in Figure 14b, the lone pair of Pb^{2+} is in this complex horizontally bisdirected and the hydrogen atoms and the lone pair of Pb^{2+} are aligned.

When the four CH$_2$ groups are also cut away (Figure 14c), a minority of the lone pair of Pb^{2+} is vertically bisdirected, whereas the majority of the lone pair is hemidirected. The lone pairs of the hydrogen atoms are still aligned with the lone pair of Pb^{2+}. Thus, we can conclude that this change in the direction and shape of the lone pair of Pb^{2+} is dictated by the hydrogen atoms that fill the dangling bonds of the removed benzene molecules. In the first and third cuts, these four hydrogen atoms point outwards from the cycle, whereas in second cut, they point inwards. When the hydrogen atoms point outwards, the distance between the hydrogen atoms is enough to have an interaction between the bisdirected lone pair of Pb^{2+} and the hydrogen atoms. However, when they point inwards, the distance between hydrogen atoms belonging to the same benzene molecule is small and the lone pair of Pb^{2+} cannot be bisdirected in this direction. Still, there is an interaction between hydrogen atoms belonging to different benzene molecules and Pb^{2+}, giving rise to a horizontally bisdirected structure.

The difference in the behaviour of the lone pair of Pb^{2+} between first and third cut can be attributed to the long distance between the remaining π bonds and Pb^{2+} so there is only a weak interaction between them, implying only a slightly bisdirected structure in the third cut. The hemidirected structure is caused by the fact that there are double bonds only on one side, similar to the structure in Figure 12.

	Pb 6p	$\Delta C(s,p)$	$\Delta H(s)$
First cut	0.91	-0.44	-0.47
Second cut	1.25	-0.86	-0.39
Third cut	0.76	-0.37	-0.39

Table 3: NBO analysis of the complex B cuts. $\Delta C(s,p)$ and $\Delta H(s)$ represent the change in the population of the s and p orbitals of all the C and the 1s orbital of all the H between the ligand with and without Pb.

The NBO analysis in Table 3 shows that the Pb 6p orbital is more occupied (implying a more efficient electron transfer) when the lone pair of Pb^{2+} is horizontal. It can be seen that in the first and third cuts,

hydrogen and carbon atoms contribute by a similar amount of electron density to fill the lone pair of Pb^{2+}, but for the second cut, the contribution from the carbon atoms is appreciably larger.

For the first and the second cut, the carbon atoms that lose the most electrons are those numerated in Figure 14 a and b. The π bonds involving these atoms align with the lone pair of Pb^{2+}. For the rest of carbon atoms, there is no significant difference in the NBO population for calculations with or without Pb^{2+}. There is also a small distinction between the hydrogen atoms: They are all identical, except those located at the end of the ligand, which donate less electron density to Pb^{2+}. Thus, it seems that the π bonds donate electrons to Pb^{2+} and then try to recover them from the hydrogen atoms. This donation is more important for the second cut.

For the third cut one can see a mixture of what happen in cut one and two. The lone pair of Pb2+ is cut into three different parts: two that could interact as a hydrogen bond like as describe above and one (the biggest one on the right) that could be explain by the repulsion of the closest carbons.

Bisdirected structures in proteins
Up to now, we have studied bisdirected structures only in fictive and symmetric model complexes. We now address the question whether such structures are possible also in biomacromolecules where Pb^{2+} sites are asymmetric?

We have studied four macromolecules from the PDB that contain Pb^{2+} ions: 1QR7[4], 2O3C[5], 1NBS[6], and 3EC8.[7] No proteins are known that require this ion for its function. Instead, Pb^{2+} has been added to help the crystallographic structure determination. The crystal structures were used directly for ELF analysis without any geometry optimisation. The system has been chosen in the way that a sphere of coordination of 8Å has been taken: no water molecule has been added and no optimisation has been done. The aim of this first part about protein is to see if a bisdirected structure could exist in an asymmetric environment. Then if one can observe this structure in small system taken in PDB then it is worth to do a QM/MM optimisation with saturated Pb^{2+}.

First, we consider the phenylalanine-regulated 3-deoxy-*D*-arabino-heptulosonate-7-phophate synthase (DAHPS; PDB code 1QR7).[4] This enzyme catalyses the stereospecific condensation of phosphoenolpyruvate and D-erythrose-4-phosphate. This reaction gives DAHP and a phosphate group. This is the first step in the biosynthetic pathway leading to aromatic compounds such as Phe, Tyr and Trp.[8]

There are four Pb^{2+} sites in this protein. Our ELF analysis shows that three of the sites are hemidirected, whereas the fourth is bisdirected. However, as can be seen from Figure 15, the lone pair of Pb^{2+} is not perfectly bisdirected; instead, a mixture of a hemi- and bisdirected structure is found. This example shows that it is possible to have a non-symmetric bisdirected lone pair. However, it is possible that this topology is linked to the fact that the structure is not optimised.
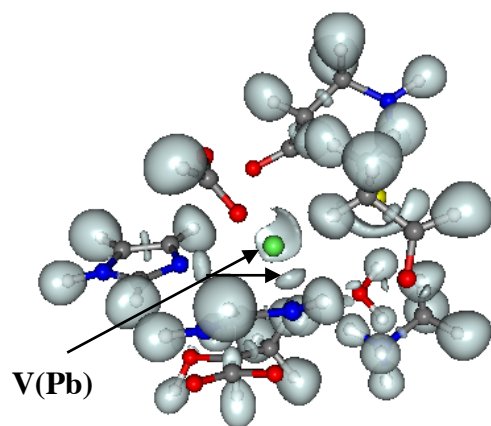
Figure 15: ELF analysis of Pb site four in the crystal structure of DAHPS (1QR7). V(Pb) is the ELF valence basin of Pb^{2+}.

The second enzyme is an apurinic/apyrimidinic endonuclease of zebrafish (PDB code 2O3C).[5] Redox regulation has been shown to play an important role in modulating the DNA binding activity of a number of transcription factors.[9] This regulation allows a higher affinity between the reduced c-Jun gene product and DNA than between oxidized c-Jun and DNA.[10] The factor responsible for reducing c-Jun is the apurinic/apyrimidinic endonuclease.

This structure contains three Pb^{2+} ions. One of the sites is shown at in Figure 16. The Pb^{2+} lone pair is clearly hemidirected. However, we can notice the presence of water molecules around Pb^{2+}. The water structure around metal ions is often dynamic. Therefore, a second ELF analysis was performed also without one of the water molecules (Figure 17), leading to a bisdirected lone pair. This indicates that there may exist a dynamics between hemi- and bisdirected structures.

Figure 16: ELF Analysis of the third Pb site in the 2O3C structure with all crystallographic water molecules.	**Figure 17: ELF Analysis of the third Pb site in the 2O3C structure with only one of the three water molecule remaining.**

The third macromolecule is ribonuclease (RNase) P, PDB code 1NBS.[6] RNase P is the only endonuclease responsible for the processing the 5' end of transfer RNA by cleaving off a precursor, leading to tRNA maturation.[11] This polyribonucleotide contains 23 Pb^{2+} sites, but some of them have only one or two ligands. 15 structures were studied by ELF analysis and bisdirected structures were observed for six of the sites as is shown in Figure 18.
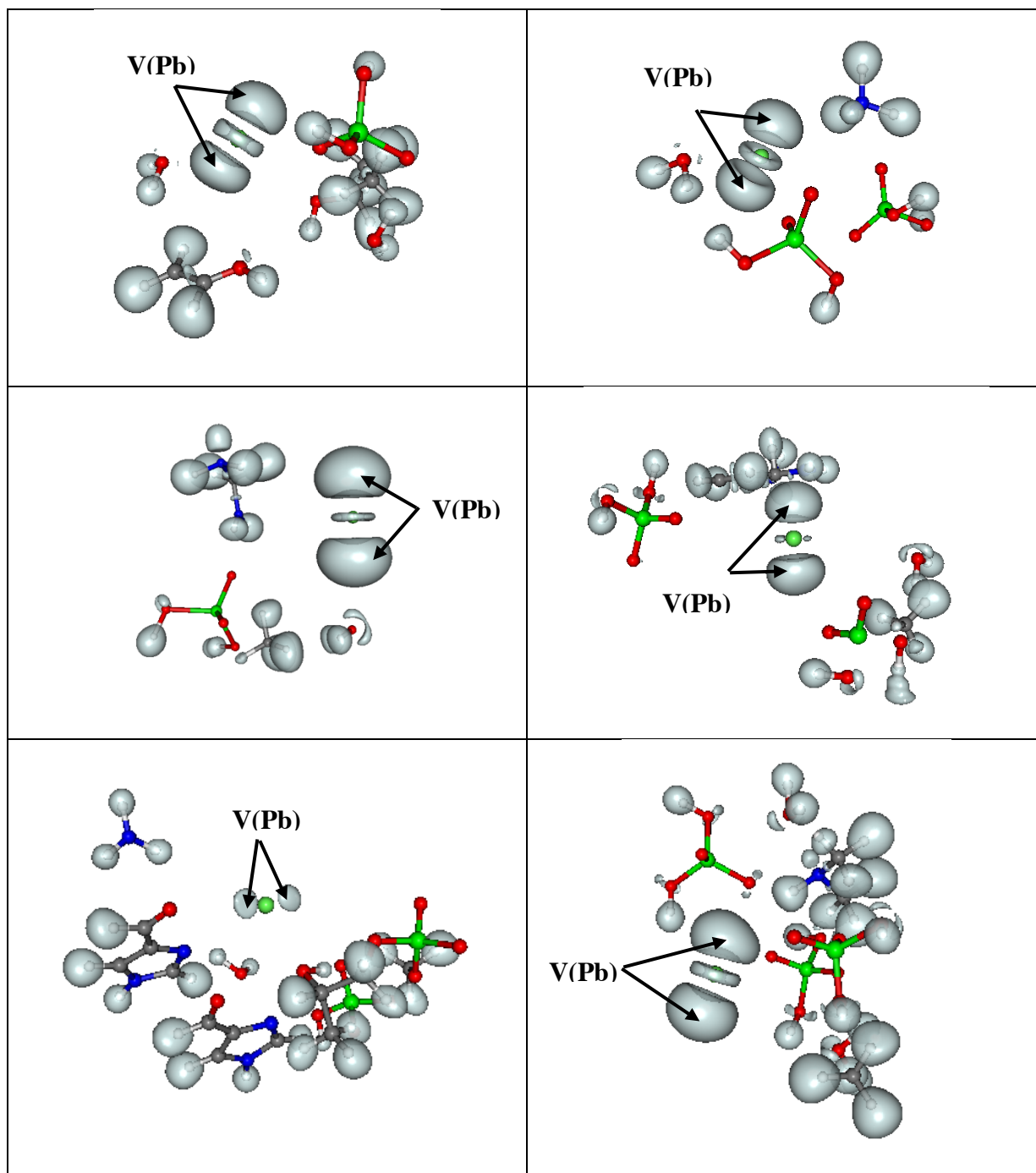

Figure 18: ELF analysis of six of the Pb sites in the crystal structure of RNase P (1NBS).[6]

One can see that the six Pb^{2+} lone pairs are nicely bisdirected despite the non-symmetric environment. It means that even if the structure would be optimised, the cation must move far away from the crystallographic position to give hemi or holodirected structures.

A problem with the interpretation of these structures is that the structure does not report any water molecules. Therefore, there is a risk that water molecules not visible in this low-resolution structure (3.15 Å) may change the topology. To test this possibility, we added two water molecules to one of the sites in Figure 18 and optimised only the water molecules (giving Pb six ligands). The optimisation was started with the two water molecules on the empty side of Pb^{2+}, opposite to the RNA groups, but after the optimisation they moved to make hydrogen bonds with the phosphate groups, but also with the lone pair of Pb^{2+}, ending up all on the same side of the Pb^{2+} ion (Figure 19). Therefore, we can conclude that the presence of water molecule does not perturb the bisdirected lone pair of Pb^{2+}.
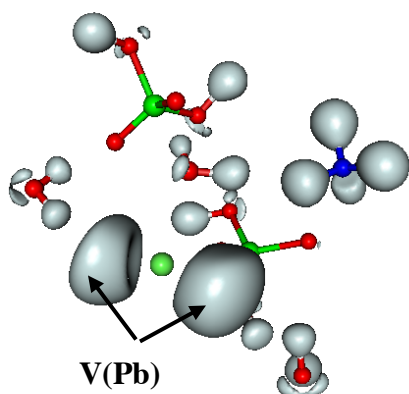

Figure 19: One of the Pb sites in 1NBS after the addition of two water molecules.

Finally, the last protein is an RA domain of FLJ10324 (RADIL), PDB code: 3EC8.[7] The structure is not properly published yet. This protein contains a single Pb^{2+} site. In this case, we used 134 atoms in the QM model, to be sure to have a well-defined environment. An ELF analysis reveals again a bisdirected structure (Figure 20).
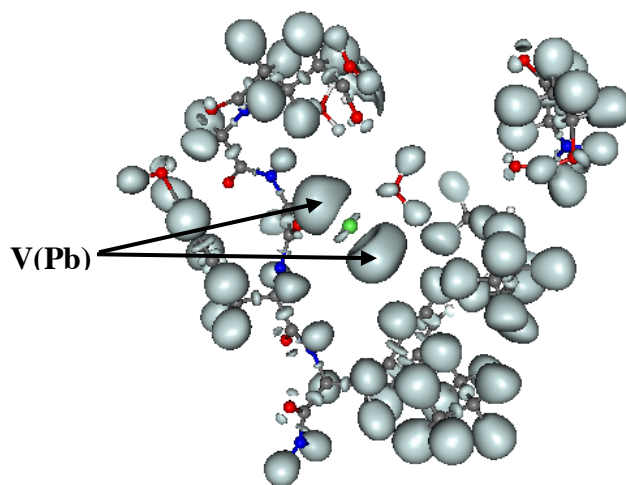

Figure 20: ELF analysis of the Pb site in the crystal structure 3EC8.

The structures presented in Figure 15–20 are not optimised and not fully saturated by water molecules. Therefore, we carried out a QM/MM calculation on the full protein 3EC8, adding three water molecules to the Pb^{2+} site. Thereby, Pb^{2+} (in pink in Figure 21) is surrounding by four water molecules and two oxygens from the protein (one back-bone carbonyl group and a Glu carboxyl group, cf. Figure 21).
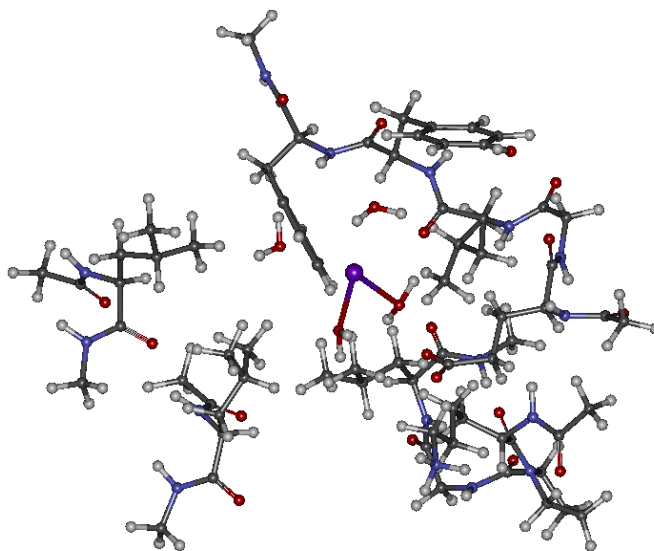

Figure 21: Surrounding of Pb^{2+} in the QM/MM calculation, representing the QM system.

The ELF analysis after the optimisations (Figure 22) show that in spite of the optimisation and the addition of water molecules, the lone pair of Pb^{2+} is still bisdirected. This strongly indicates that bisdirected structure actually may exist in biological systems.
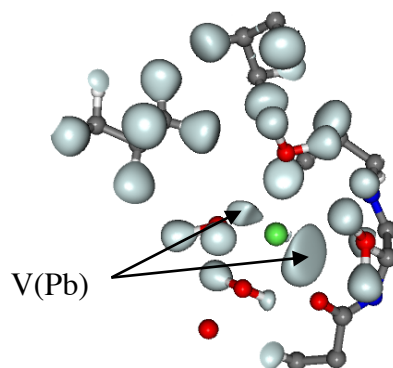

Figure 22: ELF representation of a part of the active site of 3EC8

Concluding Remarks

We have studied the occurrence of bisdirected Pb^{2+} lone pairs in various structures. First, we have studied simple symmetric model complexes to understand when bisdirected lone pairs are encountered. It seems that they arise by the repulsion of the lone pair of Pb^{2+} by other lone pairs when the ligands bind in a perpendicular way to the two hemispheres of the bisdirected lone pair. Then, the bisdirected lone pairs can arise by interactions with double bonds or lone pairs.

In the second part of this study, we have shown that bisdirected lone pairs can be found in Pb^{2+} sites in proteins and RNA. This was observed both frozen and relaxed structures, as well as when the structures were saturated with water molecules.

The results are interesting for several reasons. First, they illustrate the need of analysis methods, like ELF, to distinguish between bisdirected and holo- or hemidirected structures. Second, they emphasize that the bisdirected topology of Pb^{2+} can exist in biological environments. Now it remains to investigate whether the bisdirected structures give the Pb site unusual properties.

Methods

All ELF computations have been performed with the TOPMOD package[12] using electronic densities computed by Gaussian 03[13] at the B3LYP/SDD/6-31++G** level.[14]

The QM/MM calculations were carried out with the COMQUM program.[15,16] In this approach, the protein and solvent are split into two subsystems: The QM region (system 1) contains the most interesting atoms and is relaxed by QM methods. System 2 consists of the rest of the protein and a number of explicitly modelled water molecules. In the QM/MM geometry optimisations, system 2 was fixed at the original (crystallographic) coordinates (because we aimed at reproducing the crystal structure, improving only the structure of the Pb sites and including a number of water molecules, not discerned in the crystal structure). In the QM calculations, system 1 was represented by a wavefunction, whereas all the other atoms were represented by an array of partial point charges, one for each atom, taken from the MM libraries. Thereby, the polarization of the QM system by the surroundings is included in a self-consistent manner (electrostatic embedding).

When there is a bond between systems 1 and 2 (a junction), the hydrogen link-atom approach was employed: The QM region is truncated by hydrogen atoms, the positions of which are linearly related to the corresponding carbon atoms in the full system.[15,17]

The QM/MM energy is calculated as

$$E_{QM/MM} = E_{QM1+ptch2}^{HL} - E_{MM1,noel1}^{HL} + E_{MM12\ ,noel1}^{CL} \qquad (1),$$

where $E_{QM1+ptch2}^{HL}$ is the QM energy of the quantum system truncated by hydrogen link atoms (HL) and embedded in the set of point charges, representing system 2 (but excluding the self-energy of the point charges). $E_{MM1,noel1}^{HL}$ is the MM energy of the QM system, still truncated by HL atoms, but without any electrostatic interactions. Finally, $E_{MM123,noel1}^{CL}$ is the classical energy of all atoms with normal atoms at the junctions (carbon link atoms, CL) and with the charges of the quantum system set to zero (to avoid double-counting of the electrostatic interactions). By using this approach, which is similar to the one used in the Oniom method,[18] errors caused by the truncation of the quantum system should cancel out. Charges on all atoms in the MM system were included (except the CL atoms).

In the QM part, Turbomole[19] has been used at the DFT level with the functional TPSS[20] and the basis set ecp-78-mwb-SVP for Pb^{2+} and def2-SV(P) for the remaining atoms.[21] The resolution-of-identity (RI) approach was used to accelerate the calculations.[22,23] The QM system contained 243 atoms. For the MM

part, Amber[24] was used with the 1999 force field.[25,26] The size of the whole MM system was 5954 atoms.

Acknowledgements

References

[1] Shimoni-Livny, L.; Glusker, J. P.; Bock, C. W. *Inorg Chem* **1988**, *37*, 1853-1855.

[2] van Severen, M.-C.; Piquemal, J.-P.; Parisel, O. *Chem. Phys. Lett.* **2009**, *478*, 17-19.

[3] van Severen M.-C.;, Gourlaouen C.; Parisel, O. *J. Comp. Chem.*, **2009**, *31*, 185-194.

[4] Shumilin, I.A., Kretsinger, R.H. and Bauerle, R.H. *Structure Fold.Des.* **1999**, *7*, 865-875.

[5] Georgiadis, M.M., Luo, M., Gaur, R.K., Delaplane, S., Li, X. and Kelley, M.R. *Mutat.Res.* **2008**, *643*, 54-63.

[6] Krasilnikov, A.S., Yang, X., Pan, T. and Mondragon, A. *Nature* **2003**, *421*, 760-764.

[7] Wisniewska, M.; Lehtio,L.; Andersson, J.; Arrowsmith,C.H.; Collins,R.; Dahlgren, L. G.; Edwards, A. M.; Flodin, S.; Flores, A.; Gräslund, S.; Hammarström, M.; Johansson, A.; Johansson, I.; Karlberg, T.; Kotenyova, T.; Moche, M.; Nilsson, M.E.; Nordlund, P.; Nyman, T.; Olesen, K.; Persson, C.; Sagemark, J.; Schüler, H.; Thorsell, A. G.; Tresauges, L.; van den Berg, S.; Weigelt, J.; Welin, M.; Wikström, M.; Berglund, H., to be published, PDB structure 3EC8.

[8] Bentley, R., Crit. *Rev. Biochem. Mol. Bio.* **1990**, *25*, 307-384.

[9] a) Xanthoudakis, S. and Curran, T., *EMBO J.* **1992**, *11*, 653-665 b) Hanson, S., Kim, E., Deppert, W., *Oncogene* **2005**, *24*, 1641-1647.

[10] Abate, C., Patel, L., Rauscher, F.J.I. and Curran, T., Science **1990**, *249*, 1157-1161.

[11] a) Altman, S. And Kirsebom, L. A. *The RNA World* 351 (1999) b) Frank, D. N. and Pace, N.R. *Annu. Rev. Biochem.* **1998**, *67*, 153-180.

[12] Noury, X. Krokidis, F. Fuster, B. Silvi, B. *Comput. Chem.* **1999**, *23*, 597-604

[13] M. J. Frisch et al., Gaussian 03, Revision C.02; Gaussian Inc.: Wallingford, CT, **2007.**

[14] a) Lee, C., Yang, W., Parr, R. G. *Phys Rev B* **1988**, *37*, 785-789; b) Becke, A: D. *J Chem Phys* **1993**, *98*, 5648-5652; c)Kuechle, W., Dolg,M., Stoll, H., Preuss, H. *Mol. Phys.* **1991**, *74*, 1245-1263 f) Hay, P.J., Wadt, W. R. *J. Chem. Phys.* **1985**, *82*, 299-310; d) Schmidt, M. W., Baldridge, K., Boatz, J.A., Elbert, S.T., Gordon, M.S., Jensen, J.H., Koseki, J.S., Matsunaga, N., Nguyen, K. A., Su, S., Windus, T. L., Dupuis, M., Montgomery Jr, J. A. *J Comput Chem* **1993**, *14*, 1347-1363.

[15] Ryde, U. *J. Comput.-Aided Mol. Design* **1996**, *10*, 153-164.

[16] Ryde, U.; Olsson, M. H. M. *Int. J. Quantum Chem.* **2001**, *81*, 335-347.

[17] Reuter, NI.; Dejaegere, A.; Maigret, B.; Karplus, M. *J. Phys. Chem.* **2000**, *104*, 1720-1735.

[18] Svensson, M.; Humbel, S.; Froese, R. D. J.; Matsubara, T.; Sieber, S.; Morokuma, K. *J. Phys. Chem.* **1996**, *100*, 19357-19363.

[19] Treutler, O.; Ahlrichs, R. *J. Chem. Phys.* **1995**, *102*, 346-354.

[20] Tao, J.; Perdew, J. P.; Staroverov, V. N.; Scuseria, G. E. *Phys. Rev. Lett.* **2003**, *91*, 146401.

[21] Weigend, F.; Ahlrichs, R. *Phys. Chem. Chem. Phys.* **2005**, *7*, 3297-3305.

[22] Eichkorn, K.; Treutler, O.; Öhm, H.; Häser, M.; Ahlrichs, R. *Chem. Phys. Lett.* **1995**, *240*, 283-290.

[23] Eichkorn, K.; Weigend, F.; Treutler, O.; Ahlrichs, R. *Theor. Chem. Acc.* **1997**, *97*, 119-126.

[24] Case, D. A., Darden, T. A., Cheatham III, T. E., Simmerling, C. L., Wang, J., Duke, R. E., Luo, R., Crowley, M., Walker, R., C., Zhang, W., Merz, K. M., Wang, B., Hayik, S., Roitberg, A., Seabra, G., Kolossvary, I., Wong, K., F., Paesani, F., Vanicek, J., Wu, X., Brozell, S. R., Steinbrecher, T., Gohlke, H., Yang, L., Tan, C., Mongan, J., Hornak, V., Cui, G., Mathews, D. H., Seetin, M. G., Sagui, C., Babin, V., Kollman, P. A. Amber 10, University of California, San Francisco, 2008.

[25] Cornell, W. D.; Cieplak, P.; Bayly, C. I.; Gould, I. R.; Merz, K. M.; Ferguson, D. M.; Spellmeyer, D. C.; Fox, T.; Caldwell, J. W.; Kollman, P. A. *J. Am. Chem. Soc.* **1995**, *117*, 5179-5197.

[26] Wang, J.; Cieplak, P.; Kollman, P. A. *J. Comput. Chem.* **2000**, *21*, 1049-1074.